Ambiguity Assessment and Mitigation Approaches for the TerraSAR-X Concurrent Imaging Technique

Thomas Kraus[a], João Pedro Turchetti Ribeiro[b], Markus Bachmann[a], Renato Machado[b]
[a]Microwaves and Radar Institute, German Aerospace Center (DLR), Oberpfaffenhofen, Germany, t.kraus@dlr.de
[b]Department of Telecommunications, Aeronautics Institute of Technology (ITA), São José dos Campos, Brazil

Abstract

For TerraSAR-X, the concurrent imaging technique enables the simultaneous acquisition of scenes in two different modes and over two disjoint areas. The acquisition scheme exploits the capability to toggle the antenna configuration from pulse to pulse. A direct consequence of this interleaved acquisition scheme is the necessity to increase the azimuth sampling rate. This, in turn, affects the ambiguity performance. The paper at hand analyzes the range and azimuth ambiguity performance of the concurrent imaging technique and describes approaches to mitigate the impact of ambiguities. Additionally, the approaches are confirmed by experimental acquisitions conducted with TerraSAR-X.

1 Introduction

Traditional single-channel SAR systems acquire images in well-known imaging modes, like Stripmap, Spotlight, and ScanSAR. The spatial resolution and the scene size are characteristic parameters of each mode that need to be traded depending on the application. Additionally, only a single region of interest can be observed at a time. To overcome those limitations, next-generation SAR systems, like the proposed HRWS mission, will employ multiple channels and more sophisticated imaging modes [1, 2]. The concurrent imaging technique proposed for TerraSAR-X is a way to expand the trade space of resolution and coverage for this single-channel system [3]. Like in the scheme for the TerraSAR-X dual or quad polarization modes, the transmit and receive configurations of the radar are toggling from pulse to pulse, forming two interleaved acquisitions. As depicted in **Figure 1**, one of the images can be acquired in Stripmap mode, whereas the other can be a Staring Spotlight acquisition. Using this configuration, an area of interest can be observed with highest resolution, whereas an overview image is simultaneously produced in Stripmap mode. The concurrent imaging technique is not limited to a single area, it can also acquire data over disjoint areas. This scheme allows resolving acquisition conflicts over regions of high interest, where multiple customers like to acquire. The concurrent imaging technique opens the trade space. The acquisition of two images is possible, but with some compromises regarding the SAR performance. For example, the transmitted power is distributed over two areas and, therefore, the noise equivalent sigma zero (NESZ) performance is reduced.

The most demanding factors for the concurrent imaging technique are the timing and ambiguities and, therefore, the selection of an adequate pulse repetition frequency (PRF). The timing constraints are the same as for nominal imaging modes, as long as both parts of the concurrent acquisition are covering the same incidence angle range (cf. Figure 1). An additional timing constraint arises if disjoint areas are imaged, which depends on the location of the second scene [3]. The other demanding factor is the ambiguity performance. The PRF has to be higher than for nominal imaging modes because the effective PRF for each part of a concurrent acquisition is half the actual PRF. Therefore, relatively high PRFs are required. Such high PRFs additionally complicate the timing and reduce the achievable swath width. This paper focuses on the ambiguity performance analysis and discusses mitigation approaches.

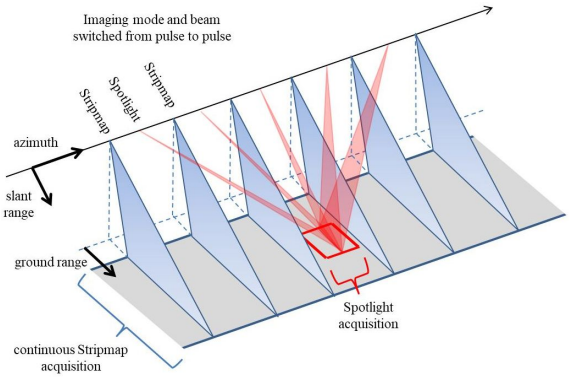

Figure 1: Concept of the concurrent imaging technique. The antenna configuration in elevation and azimuth is alternating from pulse to pulse to allow simultaneous acquisition of a Stripmap and a Spotlight scene.

The paper is structured as follows. In Section 2, the ambiguity performance of the concurrent mode is analyzed based on the Stripmap part with a focus on range and azimuth ambiguities, and a discussion of the nadir echo. In Section 3, ambiguity mitigation techniques suitable for the concurrent imaging technique are treated, and Section 4 shows experimental results. Finally, Section 5 concludes the paper.

2 Ambiguity assessment

The concurrent imaging mode acquires two images simultaneously, effectively reducing the azimuth sampling rate per image to halve the combined PRF. Therefore, on the one hand, the PRF needs to be high enough to ensure a sufficient sampling for each part of the concurrent acquisition. On the other hand, a high PRF leads to significantly increased range ambiguities. This motivates the analysis of range and azimuth ambiguities. Additionally, the nadir echo - a particular range ambiguity - is analyzed.

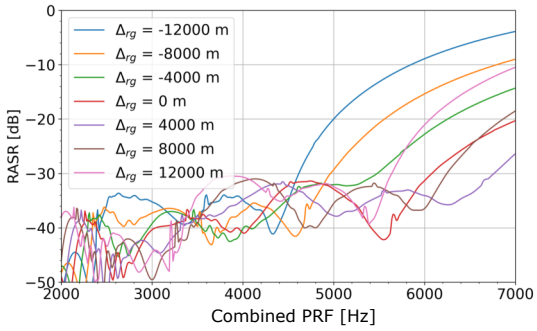

Figure 2: RASR performance for the TerraSAR-X Stripmap mode. The RASR is shown for different range target positions for the exemplary elevation beam strip_011 with an incidence angle of approximately 40°. The distance of the target under evaluation with respect to scene center Δ_{rg} is provided in the legend. In order to respect cross-interference between the modes, the *combined* PRF needs to be evaluated.

2.1 Range and azimuth ambiguities

The ambiguity performance of SAR systems is characterized by the range ambiguity-to-signal ratio (RASR) and azimuth ambiguity-to-signal ratio (AASR). For the sake of simplicity, we focus on the ambiguity performance of the Stripmap part of a concurrent acquisition. Nevertheless, the Staring Spotlight part deserves a similar analysis, as described in [3]. In **Figure 2**, the RASR performance is shown versus the PRF for the TerraSAR-X Stripmap beam strip_011. To evaluate the figure, the *combined* PRF which is tiwce the *effective* PRF needs to be used, as there is cross-interference between the modes of a concurrent acquisition. For a PRF below 5000 Hz the RASR is better than -20 dB. For higher PRFs, the RASR is degrading especially for targets at the range scene edges.

In **Figure 3**, the AASR performance for the Stripmap part is shown for different processed azimuth bandwidths pBW. To evaluate the figure, the *effective* PRF needs to be used, as it is the sampling frequency in azimuth direction for each part of a concurrent acquisition. For a given PRF, selecting the processed azimuth bandwidth provides certain flexibility. It is possible to trade azimuth ambiguity performance against azimuth resolution. To achieve an AASR of -20 dB at a processed azimuth bandwidth of 2750 Hz (cyan line in Figure 3) an effective PRF of at least 3200 Hz is necessary. This would mean a combined PRF of 6400 Hz. Comparing the results of Figure 2 and 3, it is clear that the concurrent imaging mode is compromising the ambiguity performance for acquiring two acquisitions in parallel.

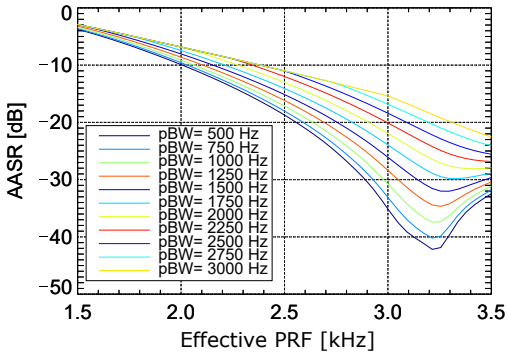

Figure 3: AASR performance for the TerraSAR-X Stripmap mode. The AASR for different processed azimuth bandwidths is shown. For the evaluation, the *effective* PRF needs to be used.

2.2 Nadir echo

The Nadir echo is the signal received from the area with the closest distance to the satellite. The intensity of the nadir echo can be strong because of the short distance and the specular reflection. Typically, the nadir echo manifests as a bright line in SAR images [4]. Usually, spaceborne SAR systems like, e.g., TerraSAR-X are designed to avoid the nadir interference by properly selecting of the PRF [5]. However, in the case of concurrent imaging, the usable PRF range is already very limited due to ambiguity and system considerations, and this additional constraint complicates the selection of an appropriate PRF for many scenes. Therefore, a relaxation of the nadir interference constraint is highly desirable and will be assessed in Section 3.2.

3 Ambiguity mitigation

In literature, many approaches to mitigate or avoid ambiguities are discussed, like azimuth phase coding [6], the exploitation of several azimuth channels [7], and the use of waveform encoding [8, 9]. Because of the characteristics of the concurrent imaging technique, we like to focus on spectral diversity and waveform encoding here.

3.1 Spectral diversity

The use of waveforms with no spectral overlap would be an option to suppress the cross interference between both images of a concurrent acquisition. However, partially overlapping spectra enable trade between range ambiguity performance and range resolution. On the one hand,

ambiguities are improving as the spectral overlap reduces. Additionally, the SNR is improving with reduced bandwidth. On the other hand, the resolution is degrading. In **Figure 4**, the available range bandwidth filters of the TerraSAR-X radar instrument are shown, providing 100 MHz, 150 MHz, and 300 MHz bandwidth. Depending on the transmitted waveform, the smallest possible receive bandwidth is used to reduce the recorded amount of data and the data rate of the mass memory. Those parameters are limiting factors for the achievable scene size for the TerraSAR-X high-resolution modes [10]. The red and blue arrows represent an exemplary transmit bandwidth of 50 MHz for the Stripmap and 175 MHz for the Staring Spotlight part of the acquisition, respectively. Assuming the same transmit power for the Stripmap and the Staring Spotlight pulses, a 3 dB improvement of the Stripmap interference within the Staring Spotlight is expected compared to a full spectral overlap because only half the Stripmap bandwidth is overlapping with the Staring Spotlight bandwidth. However, as depicted in **Figure 5**, the signals are weighted by a (generalized) Hamming window with α= 0.6, and, therefore, the interference is reduced further. The Staring Spotlight signal interfering with the Stripmap signal is reduced by -12.1 dB compared to a complete spectral overlap without windowing. Comparing the spectral diversity approach shown in Figure 5 with the standard bandwidth settings of the concurrent imaging mode (100 MHz for Stripmap and 300 MHz for Staring Spotlight), as shown in **Figure 6** an improvement in the ambiguity levels of 3.7 dB is expected.

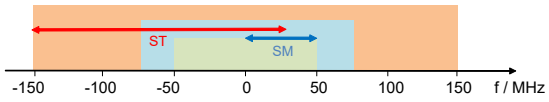

Figure 4: Range frequency filter bandwidths of the TerraSAR-X instrument in the receiver. There are three filters available onboard: 100 MHz, 150 MHz, and 300 MHz, shown in green, blue, and red colors, respectively. The red and blue arrows highlight a possible transmit bandwidth setting used for the experiment, as shown in Section 4.

3.2 Waveform encoding

The inherent characteristic of the concurrent imaging technique to toggle the antenna configuration from pulse to pulse suggests altering the used waveform in a similar fashion. By using up and down chirp variation, a defocusing of the echos of the other acquisition can be achieved respectively [8]. This is of great value as the first range ambiguity is dominant in many cases. It is the closest one and, therefore, prone to relatively high gain of the elevation antenna pattern. Actually, not only the first but every odd order of ambiguity is experiencing defocusing. This is of special interest considering the nadir echo, as it is also a dominant source of interference. Using up and down chirp variation, the reception of nadir interference can be acceptable as it no longer focuses on a bright line in the image. This is possible, if the order of the nadir ambiguity is odd. This approach brings back some flexibility in selecting PRFs which is highly valuable, especially for the concurrent imaging approach.

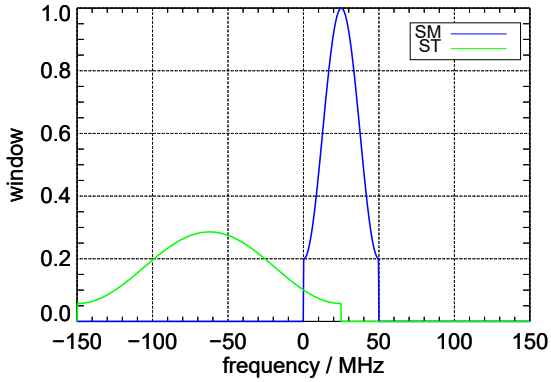

Figure 5: Normalized spectrum of the Stripmap and Spotlight signals shown in Figure 4 weighted by a Hamming window with α= 0.6 in blue and green, respectively.

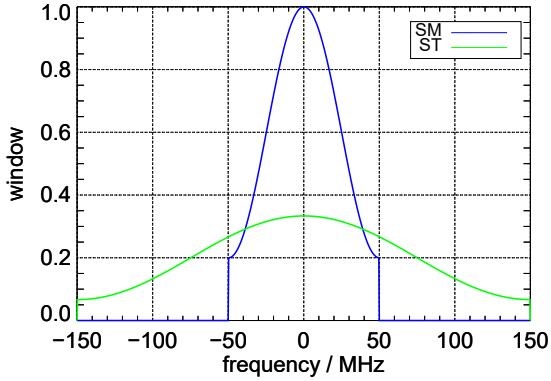

Figure 6: Normalized spectrum of the Stripmap and Spotlight signals used for standard concurrent imaging weighted by a Hamming window with α= 0.6 in blue and green, respectively.

Using up and down chirp variation is beneficial for point-like targets as they are not focusing. However, the approach is not sufficient for distributed targets, as the energy of the targets is not filtered out but is still present in the image [8]. Even if not focused, the nadir echo can be recognizable. In this case, the dual-focus postprocessing approach described in [11], [9] can be exploited to remove the power of the nadir echo before the focusing of the intended image.

4 Experimental results

To assess range ambiguities, acquisitions employing the concurrent imaging technique close to the city of Buenos Aires, Argentina, have been commanded, acquired and processed. In **Figure 7**, three Stripmap images are shown. The left one is the Stripmap part of a concurrent acquisition performed on 2020-09-24 with elevation an-

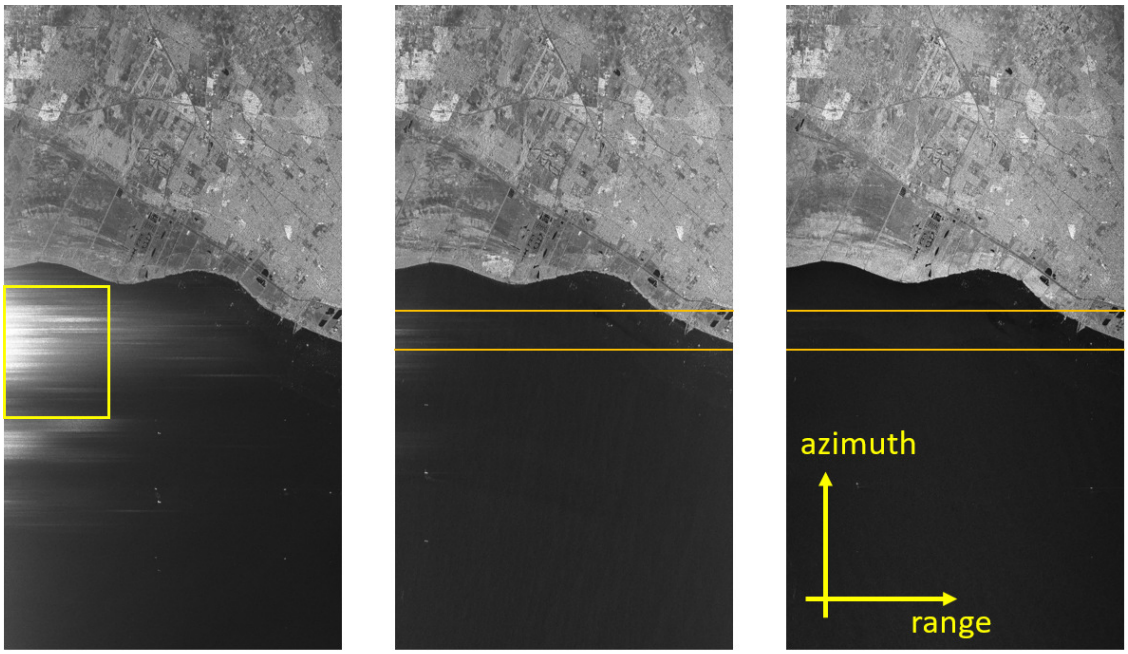

Figure 7: Stripmap images of three concurrent acquisitions close to the city of Buenos Aires, Argentina. The left image was acquired on 2020-09-24 using elevation beam strip_011. This beam results in reduced antenna gain in near range, leading to the exaggeration of ambiguous signals here. The middle image was acquired on 2020-10-16, using elevation beam tanDEM_a1_040. This beam ideally illuminates the scene and provides an image with significantly reduced ambiguities. This beam would be the choice for an operational acquisition. The right image was acquired on 2021-03-30, using elevation beam tanDEM_a1_040 and the bandwidth settings described in Section 3.1 and shows even lower ambiguities.

tenna beam strip_011. This elevation beam was selected in order to provoke the appearance of range ambiguities in near range, as the antenna gain in near range is degraded compared to a nominal acquisition. The beam is not centered over the receive echo window. During processing, the antenna pattern compensation enhances the signal energy in the near range area and leads to the dominant appearance of ambiguities. A high ambiguous power especially close to the center in azimuth direction is notable, as highlighted by the yellow box. For comparison purposes, the same area was acquired on 2020-10-16 with elevation beam tanDEM_a1_040, as shown in the middle of Figure 7. This scene can serve as a reference.

As discussed in Section 3.1, reduced range ambiguity power is expected when acquiring the same area with an adjusted waveform. The resulting image is shown on the right. A reduction of the range ambiguity power at near range can clearly be observed. To assess this in more detail, a cut in range direction is shown in **Figure 8**. The curves are an average over 1252 range lines in the azimuth center of the images as indicated by the orange lines in Figure 7. The blue curve corresponds to the middle image of Figure 7, using the conventional bandwidth setting. The green curve corresponds to the right image, for which the spectral diversity approach is employed. A reduction of the ambiguity power is visible, especially in near range. Overall, a reduced noise level due to the reduced bandwidth is visible in the sea areas. The right part of both curves corresponds to the landmasses in far range, as shown in Figure 7. A drawback is a degradation of the slant range resolution from 1.8 m to 3.6 m, because of the reduced bandwidth.

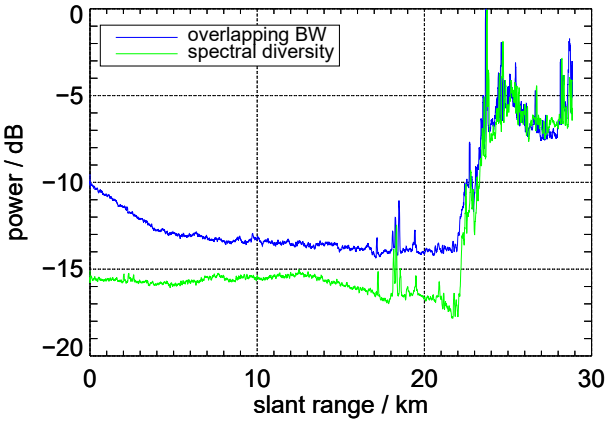

Figure 8: Normalized signal power of a cut in range direction. The data is averaged over 1252 range lines around the azimuth center of the image. The blue curve corresponds to the middle image of Figure 7 using an optimized elevation beam and nominal bandwidth settings. The green curve corresponds to the right image of Figure 7 using the spectral diversity approach described in Section 3.1. An improvement in the ambiguity power is visible, especially in the near range and the noise level is lower because of the reduced bandwidth.

To analyze the signal characteristics of the ambiguous signal, spectrograms of single raw data range lines close to the azimuth center position are derived, as shown in **Figure 9**. The left spectrogram corresponds to the acquisition depicted in the center of Figure 7 and the right one to the right acquisition, respectively. In both spectrograms, a dominant down chirp signal is visible. In both cases, the chirp slope and the chirp rate correspond to the waveform used for the Staring Spotlight part of the concurrent acquisition. Since the spectrum of the Staring Spotlight part is only partially overlapping with the bandwidth used for the Stripmap mode, no down chirp signal is visible in the upper part of the right spectrogram when employing the waveform diversity approach. The ambiguous signal is not focusing in range. Still it is smeared, because the images in Figure 7 are focused using the matched filter for the waveform employed for the Stripmap mode.

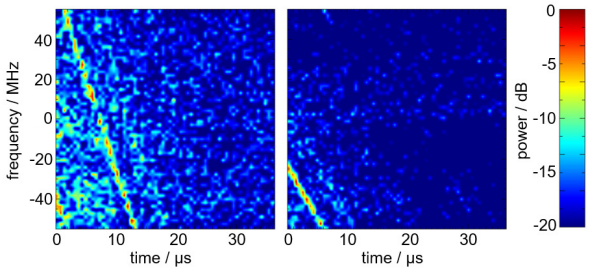

Figure 9: Spectrograms of a single range line at the azimuth center position. The left spectrogram corresponds to the center image in Figure 7, whereas the right spectrogram corresponds to the right acquisition. Both spectrograms are normalized to their respective maximum value. In both, a dominant down chirp signal is visible.

In order to identify the source of the ambiguous signal, the lower part of the spectrum (cf. Figure 4) can be focused with a matched filter according to the signal characteristics of the Staring Spotlight transmit signal. Additionally, the slant range according to the expected ambiguous position needs to be respected during azimuth focusing. In **Figure 10**, a Google Earth overlay of the Stripmap part of the concurrent acquisition is shown. The right orange box highlights the region where the strongest ambiguous signal is expected. The red framed image is the same part of the raw data (orange frame) but processed with matched filters respecting the signal characteristics of the ambiguity. As the zoom-in on the lower part of Figure 10 shows, the ambiguous signal is focusing. The dominant target, in this case, is a building perfectly oriented in flight direction, forming a very bright target. It is highlighted with orange ellipses in the SAR image and the optical image from Google Earth. This high backscatter is causing the ambiguities recognizable in the left and the center images of Figure 7. The right image is characterized by vanishing ambiguities because the major part of the ambiguous signal is removed by filtering according to the spectral diversity approach. The remaining ambiguous energy is smeared in the range direction due to the waveform encoding and therefore visually disappears.

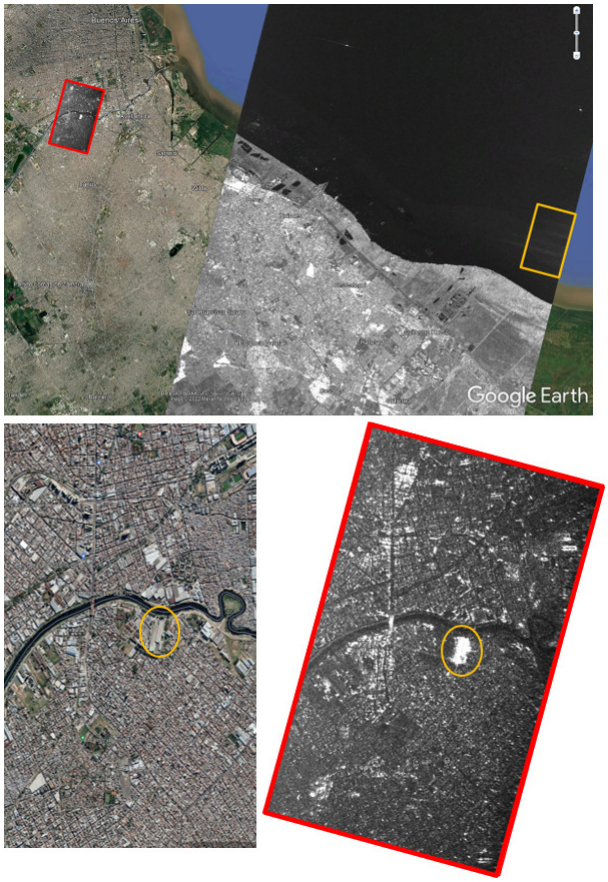

Figure 10: Google Earth overlay of the Stripmap part of the acquisition employing spectral diversity. The right orange box in the upper image indicates the region where the most ambiguous power is expected. The left red box is derived from this part of the same dataset but processed with a matched filter fitting the ambiguous signal and an adjusted slant range according to the expected location of the ambiguity. The lower images are zoom-ins on the ambiguous image (right) and the optical counterpart from Google Earth. The orange ellipse highlights a dominant target in the scene.

In **Figure 11**, the up and down chirp waveform encoding approach is highlighted for nadir signals. The upper right image shows the Google Earth overlay of two Stripmap images of one concurrent acquisition acquired 2021-05-02 close to the island of Mauritius. The left image is the nominally focused first swath. The center image is the same raw data but focused with the opposite chirp slope. Here all targets within the scene are not focused in range. However, the nadir signal is focusing as highlighted by the orange box and the cut in range direction shown on the lower right. The nadir signal is not focusing in the actual image, because the intended swath has an even echo index, whereas the nadir signal has an odd.

In this example the nadir echo can be tolerated, since the unfocused echo is not disturbing the image. In case the nadir echo would be stronger the dual focus post pro-

cessing technique [11] can be employed to remove the focused nadir echo and subsequently focus the intended scene as demonstrated for TerraSAR-X [9] and ICEYE [12].

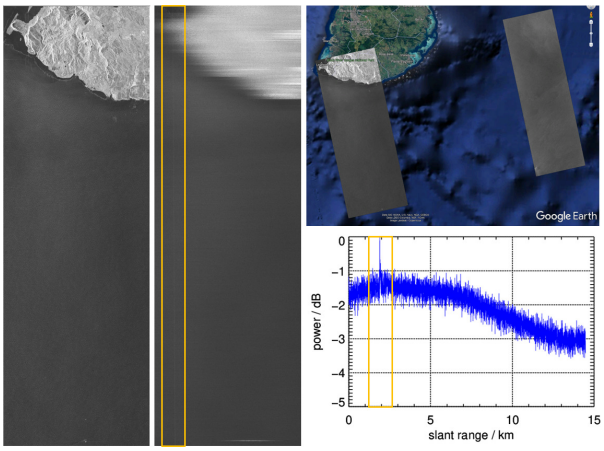

Figure 11: Concurrent acquisition close to Mauritius consisting of two Stripmap images represented as Google Earth overlay (upper right). The first swath nominally focused (left) and focused with the opposite chirp slope (center). Since the nadir echo is coming from the other waveform, the nadir is focusing here, as highlighted with the orange box and range profile (lower right).

5 Conclusions

The paper addresses one of the major challenges of the concurrent imaging technique, namely ambiguities. Range and azimuth ambiguities, as well as nadir interference, as a special kind of range ambiguity, are discussed. Methods to improve the ambiguity performance are introduced. The use of up and down chirp waveform encoding and the approach of spectral diversity were derived, assessed, and show promising results. Two experiments showcase the origin of the ambiguous signal and its suppression using waveform encoding and spectral diversity. The suppression of nadir interference using waveform encoding was demonstrated, and the mitigation of nadir interference using dual focus post processing was outlined. The discussion in this paper is focused on the concurrent imaging technique of TerraSAR-X. However, the methods are also applicable for other SAR modes and missions.

References

[1] J. Janoth, M. Jochum, L. Petrat, and T. Knigge, "High resolution wide swath - the next generation X-band mission," in *Proc. IEEE Geosci. Remote Sens. Symp. (IGARSS)*, 2019.

[2] J. Mittermayer, G. Krieger, M. Villano, and A. Moreira, "A novel MirrorSAR concept for augmenting the next german synthetic aperture radar mission HRWS with single-pass interferometry," in *Proc. of the 13th IAA Symposium on Small Satellites for Earth Observation*, 2021.

[3] T. Kraus, J. P. Turchetti, M. Bachmann, U. Steinbrecher, and C. Grigorov, "Concurrent imaging for TerraSAR-X: Wide-area imaging paired with high-resolution capabilities," *IEEE Trans. Geosci. Remote Sens.*, vol. 60, pp. 1–14, 2022.

[4] J. Balkoski and F. Bordoni, "Nadir echo properties, a study based on TerraSAR-X data," in *Proc. 20th Telecommunications Forum (TELFOR)*, 2012, pp. 420–423.

[5] J. Mittermayer, M. Younis, R. Metzig, S. Wollstadt, J. Márquez-Martínez, and A. Meta, "TerraSAR-X system performance characterization and verification," *IEEE Trans. Geosci. Remote Sens.*, vol. 48, no. 2, pp. 660–676, 2010.

[6] J. Dall and A. Kusk, "Azimuth phase coding for range ambiguity suppression in SAR," in *Proc. IEEE Geosci. Remote Sens. Symp. (IGARSS)*, 2004, pp. 1734–1737.

[7] G. Krieger, N. Gebert, and A. Moreira, "Unambiguous SAR signal reconstruction from nonuniform displaced phase center sampling," *IEEE Geosci. Remote Sens. Lett.*, vol. 1, no. 4, pp. 260–264, 2004.

[8] J. Mittermayer and J. M. Martínez, "Analysis of range ambiguity suppression in SAR by up and down chirp modulation for point and distributed targets," in *Proc. IEEE Geosci. Remote Sens. Symp. (IGARSS)*, vol. 6, 2003, pp. 4077–4079.

[9] S.-Y. Jeon, T. Kraus, U. Steinbrecher, G. Krieger, and M. Villano, "Experimental demonstration of nadir echo removal in SAR using waveform diversity and dual-focus postprocessing," *IEEE Geosci. Remote Sens. Lett.*, pp. 1–5, 2021.

[10] T. Kraus, B. Bräutigam, J. Mittermayer, S. Wollstadt, and C. Grigorov, "TerraSAR-X staring spotlight mode optimization and global performance predictions," *IEEE J. Sel. Topics Appl. Earth Observations Remote Sens.*, vol. 9, no. 3, pp. 1015–1027, 2015.

[11] M. Villano, G. Krieger, and A. Moreira, "Nadir echo removal in synthetic aperture radar via waveform diversity and dual-focus postprocessing," *IEEE Geosci. Remote Sens. Lett.*, vol. 15, no. 5, pp. 719–723, 2018.

[12] O. Dogan, V. Ignatenko, D. Muff, L. Lamentowski, M. Nottingham, A. Radius, P. Leprovost, and T. Seilonen, "Experimental demonstration of a novel end-to-end SAR range ambiguity suppression method," in *2022 IEEE Radar Conference (RadarConf22)*, 2022, pp. 1–6.